Small Animal Imaging by Single Photon Emission Using Pinhole and Coded Aperture Collimation

F. Garibaldi, R. Accorsi, M. N. Cinti, E. Cisbani, S. Colilli, F. Cusanno, G. De Vincentis, A. Fortuna, R. Fratoni, B. Girolami, F. Ghio, F. Giuliani, M. Gricia, R. Lanza, A. Loizzo, S. Loizzo, M. Lucentini, S. Majewski, F. Santavenere, R. Pani, R. Pellegrini, A. Signore, F. Scopinaro, and P. P.Veneroni

***Abstract*—The design of detectors for radio-imaging of small animals is challenging because of the high spatial resolution required, possibly coupled with high efficiency to allow dynamic studies. Spatial resolution and sensitivity are difficult to attain at the same time with single photon imaging techniques because collimators define and limit performance. In this paper we first describe a simple desktop gamma imager equipped with a pinhole collimator and based on a pixellated NaI(Tl) scintillator array coupled to a Hamamatsu R2486 PSPMT. The limits of such a system as well as the way to overcome them in future systems is shown next. Better light sampling at the anode level would allow better pixel identification for a higher number of pixels, which is one of the parameters defining image quality and improving spatial resolution. The performance of such a design is compared with other designs using other PSPMT types with different light sampling schemes at the anode level. Finally, we show how the substitution of the pinhole collimator with a coded aperture collimator can result in a substantial improvement in system sensitivity while maintaining very good spatial resolution, possibly at a sub-millimeter level. Calculations and simulations of a particular solution show that sensitivity can improve by a factor of nearly 30.**

***Index Terms*—Nuclear imaging, scintillation detectors, sensitivity, spatial resolution.**

I. Introduction

THE recent availability of genetically modified mice has generated a rapid growth of interest in radio imaging of small animals, because it enables a wide range of human diseases to be studied in animal models. Indeed radio-labeling of small molecules, antibodies, peptides, and probes for the gene expression enables molecular imaging *in vivo*, but only if a suitable imaging system is available. The design of imaging systems for small animals is very challenging because of the often concurrent requirements of high spatial resolution and sensitivity. Positron emission tomography (PET) has the advantages of high sensitivity and high spatial resolution [1]. Nevertheless, PET has intrinsic limitations in terms of spatial resolution and suffers from increased complexity and cost. For this reason different groups [2]–[4] have advocated the use of single photon emission computed tomography (SPECT), which is in principle simpler, less expensive, and can make use of a large variety of available labeled molecules. The spatial resolution of single photon systems is limited to the sum in quadrature of intrinsic resolution of the detector and bore size if parallel hole collimators are used, but significant improvements are possible if pinhole collimators are used. The major drawback is limited sensitivity of such system. Although calculations and simulations show that reasonable count rates can be obtained [2], in dynamic studies higher sensitivity is needed [4]. It has been shown [4], [6] that it is possible to increase sensitivity by careful design of the collimator system. For example, a coded aperture technique can provide much higher sensitivity while maintaining sub-millimeter spatial resolution. A collaboration started among the Italian National Institute of Health (Istituto Superiore di Sanitá), Rome, Italy; the Experimental Medicine Department of Rome University La Sapienza, Rome, Italy; the Massachusetts Institute of Technology, Cambridge; and the Children's Hospital of Philadelphia, PA for the study and realization of an optimized single photon small animal imaging system to be used for both static and dynamic studies. We have performed calculations in order to evaluate the performance of the different detector setups in terms of spatial resolution and sensitivity for different field of view (FOV) sizes. The results are similar to what can be found in the literature [2]–[4]. The well-known tradeoff between FOV, sensitivity, and spatial resolution is evident. A compact prototype gamma camera has been built which, in combination with a pinhole collimator, allows for high resolution in vivo SPECT imaging. The limits of such a system have been studied with possible ways to overcome them. A coded aperture collimator was designed, built, and tested. It was coupled with a high resolution scintillation detector to build a mini gamma camera with high efficiency and the high spatial resolution needed for small animal imaging. High sensitivity and sub-millimeter spatial resolution have been obtained at the same time in the dedicated small animal imager. This would open the possibility for dynamic high resolution animal studies.

Manuscript received June 16, 2005; revised June 16, 2005.

F. Garibaldi, E. Cisbani, S. Colilli, F. Cusanno, A. Fortuna, R. Fratoni, B. Girolami, F. Ghio, F. Giuliani, M. Gricia, A. Loizzo, S. Loizzo, M. Lucentini, F. Santavenere, and P. Veneroni are with Istituto Superiore di Sanitá and INFN, Roma1, Rome I00161, Italy (e-mail: franco.garibaldi@iss.infn.it).

R. Accorsi is with the Division of Nuclear Medicine, Department of Radiology, The Children's Hospital of Philadelphia, PA USA.

M. N. Cinti, G. De Vincentis, R. Pani, and R. Pellegrini are with Dipartimento di Medicina Sperimentale, Universita' La Sapienza—Rome, Rome, Italy.

R. Lanza is with the Department of Nuclear Engineering, Massachusetts Institute of Technology, Cambridge, MA USA.

S. Majewski is with Jefferson Laboratory, Newport News, VA USA.

A. Signore and F. Scopinaro are with Dipartimento di Scienze Radiologiche, Universita' La Sapienza, Rome, Italy.

Digital Object Identifier 10.1109/TNS.2005.851428

II. Equipment

We have used two arrays of pixellated NaI(Tl) crystals (Saint Gobain Crystals and Detectors), the first one 56×56 mm^2 with 1.25×1.25 mm^2 pixel size (1.5 mm pitch), and the second 48×48 mm^2 in size, with 1.8×1.8 mm^2 (2 mm pitch). The

Fig. 1. Two detector setups using different photodetectors. At left: NaI(Tl) pixellated array ($1.8 \times 1.8 \times 6$ mm^3) coupled with R2486 Hamamatsu PSPMT using pinhole collimator. At right: The same system but using H8500 PSPMT as photodetector.

thickness of both arrays was 6 mm. The optical separation between pixels is made of 0.25 mm white epoxy septa. The thickness of the optical glass window attached to the arrays is 3 mm.

The scintillator arrays were coupled to several different Hamamatsu PSPMTs: R2486, R5900 (M16 and M64), and the H8500. The R2486 is the first generation of Hamamatsu PSPMTs, characterized by an intrinsic spread of charge, a circular shape (3″ in diameter), and a glass window 3.2 mm thick. The M16 (M64) PSPMT has a 0.8 mm glass window, 16 (64) 0.5 mm apart anode pads in a 4×4 (8×8) array of 4×4 mm^2 (2×2 mm^2), respectively. In both PSPMTs, the active area corresponds to the anode area (18×18 mm^2). Charge multiplication is achieved with 12 metal channel dynode stages. Charge spread is much smaller than in the first generation R2486 PSPMT. The Hamamatsu H8500 Flat panel PMT has an external size of $52 \times 52 \times 14.7$ mm^3, the photocathode is bialkali, and 12 stages metal channel dynode are used as an electron multiplier. 8×8 matrix anode pads (64 channels) are used for a position sensitive function in which each individual pad has 6 mm pitch. The peripheral dead zone is reduced to 1.5 mm (with 0.5 mm as final goal), so the overall active area is 49×49 mm^2. The maximum PMT gain is about 3×10^6. The anodes were directly connected to CAMAC ADCs, and sent to a PC, in list mode, through a SCSI interface. The digitized individual anode signal amplitudes were recorded in a list mode on a PC. The position of each scintillation event was calculated with a digital centroid technique applied to the individual anode amplitudes. Parallel hole as well as pinhole and coded aperture collimators were used. The parallel hole collimator was a standard general purpose lead collimator (hole diameter 1.5 mm, hole length 22 mm, and septa thickness 0.2 mm). The two tungsten pinhole collimators had a knife aperture with an angle of 60 degrees and hole diameters 1 and 0.67 mm. Fig. 1 shows components of the detector setup used.

III. Methods

Flood field irradiation was performed for all detector setups with a point source ($\sim$50 μCi, ^{57}Co ($E_\gamma = 122$ keV)) placed at $\sim$2 m from the detector. Measurements with the parallel hole collimator were done with the source at the collimator surface. Measurements with pinhole collimators were performed for different magnification factors (M) and, accordingly, field of views (FOV). Magnification factors between $\sim$3 and $\sim$7 were used. For $M \sim 3$, the detector to pinhole distance (a) was 44 mm, while the pinhole object distance (b) was 14 mm. In the case of $M \sim 7$, the distances were a =44 mm and b =6.5 mm. The measurement with coded aperture collimator was performed with a =44 mm and b =14 mm.

We have analyzed the basic detector parameters (number of pixels, pixel separation, and type of collimation) of different gamma-cameras built with different scintillators, phototubes, and collimators. The aim was to understand the role of these parameters on spatial resolution and sensitivity, the key parameters for the small animal imaging. Spatial resolution depends on the pixel size and precision of their identification/separation, depending in turn on light sampling and consequently on the dimension (granularity) of the photodetector's anode readout elements (pads, strips, etc). Two other important parameters are sensitivity, which depends on the collimation, and energy resolution, which is not critical when imaging small animals because of reduced object–detector distance with respect to the humans.

IV. Results

A. Parallel Hole Versus Pinhole Collimator

Fig. 2 shows that spatial resolution is better with the 1 mm pinhole collimator (1.5 mm compared with 2.4 mm FWHM), but the sensitivity is lower by a factor of 5. Measurements were performed using the R2486 coupled to the 1.8×1.8 mm^2 scintillator.

B. Scintillator Detector Pixel and Anode Pixel Size

Figs. 3–7 show the comparison of different detector layouts: two arrays of pixellated NaI(Tl) scintillators coupled to the R2486 and two other PSPMTs (R5900-M16 and R5900-M64),

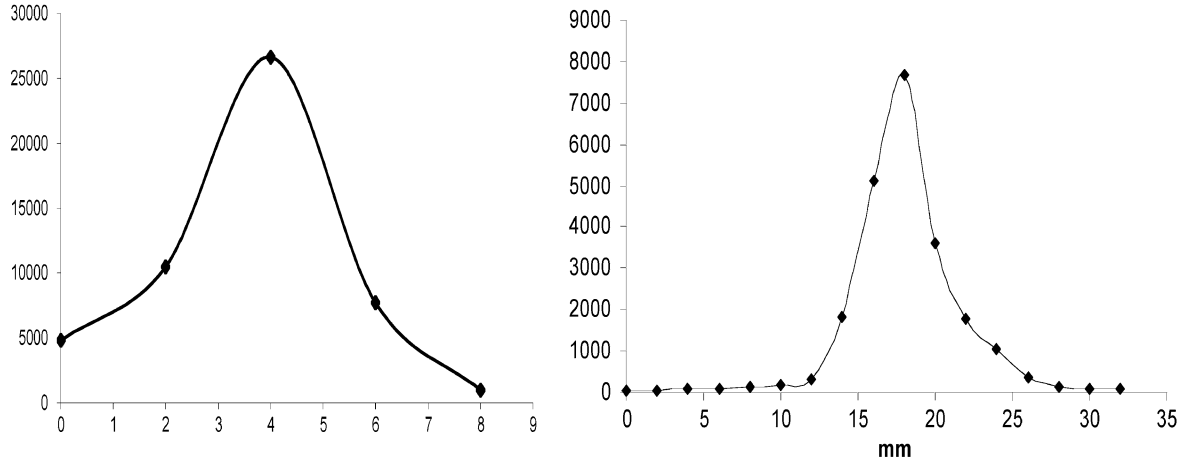

Fig. 2. Measured spatial resolution, using a point source (122 keV, 1 mm diam), for a standard parallel hole collimator (left, hole diameter 1.5 mm, hole length 22 mm, septa thickness 0.2 mm) and a pinhole collimator (right, 1 mm aperture). NaI(Tl) array ($1.8 \times 1.8 \times 6$ mm^3), R2486 PSPMT. In both measurements, the distance between source and collimator is 7 mm. When deconvolved with the source dimension, the result is, respectively, 2.0 mm and 1.2 mm.

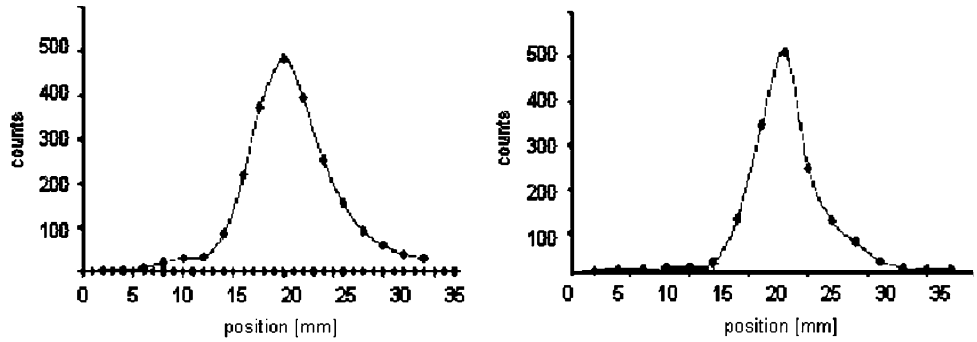

Fig. 3. Measured as full-width at half-maximum of reconstructed position distribution. Left: $M = 3$, spatial resolution = 1.3 mm. Middle: $M = 7$, spatial resolution = 1.1 mm, both obtained for NaI(Tl) array ($1.8 \times 1.8 \times 6$ mm^3) and R2486 PSPMT.

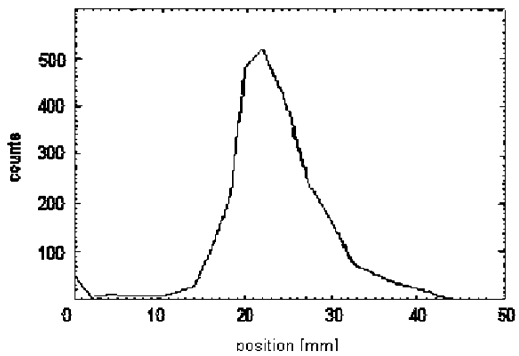

Fig. 4. Spatial resolution using a point source (122 keV, 1 mm diam), scintillator array (NaI(Tl) $1.8 \times 1.8 \times 6$ mm ^{3}). Tungsten pin hole (aperture = 0.67 mm), R2486. $M = 7$ FWHM = 1.1 mm. The spatial resolution is improved with respect to the 1 mm aperture pinhole.

having different structures, namely better light sampling capability at the anode level and two pinhole collimators with different apertures (1 mm and 0.67 mm).

The results can be summarized as follows.

- Increasing magnification improves spatial resolution (Fig. 3). The drawback is the smaller FOV.
- Spatial resolution improves with decreasing pinhole aperture (Fig. 4 and Table I).
- The pixel identification is poor for the R2486 when coupled to the $1.8 \times 1.8 \times 6$ mm^3 scintillator array and very poor for the $1.25 \times 1.25 \times 6$ mm^3 scintillation array [Figs. 5(a) and (d)]. This is probably due to the (relatively) large spread of charge, which contributes to an insufficient light sampling capability for accurate pixel identification. We take the peak/valley ratio as quality parameter for the accuracy of pixel identification.
- Better performance with M16 and M64 were expected and have been obtained [Figs. 5(b), (c), (e), and (f) and Table I]. In fact, it is known that the charge spread is much smaller in the new generation of Hamamatsu PSPMTs.
- No great advantage is obtained by reduction of the anode pixel size from 4×4 mm^2 (M16) to 2×2 mm^2 (M64).
- Pixel identification and intrinsic spatial resolution improves with smaller anode photodetector dimensions.

Careful investigation has to be made in the choice of the anode pixel size of the photodetector, taking into account also that the magnifying geometry makes the intrinsic spatial resolution less important, and considering other practical aspects such as the total number of readout channels, for example. We estimate the 3×3 mm^2 anode pixel size to be the best compromise. Moreover, the R5900-M16 and R5900-M64 PSPMTs have a small active area. In principle, arrays of these PSPMTs can be built to have a practically useful detector area, but this

TABLE I
SUMMARY OF THE PERFORMANCES OF THE DIFFERENT SYSTEMS TESTED

Collimator	Scintillator array (NaI (Tl))	PSPMT	Hole dimension (mm)	Spatial resolution (mm)	Magnification	Peak / valley
Parallel hole	1.8 x 1.8x 6 mm^3	R2486	1.2	2.0	1	1.4
Pinhole	1.8 x 1.8 x 6 mm^3	R2486	1	1.2	7	1.4
Pinhole	1.8 x 1.8 x 1.8 mm^3	R2486	1	1.3	3	1.4
Pinhole	1.25 x .25 x 6 mm^3	R2486	1	1.2	7	0.7
Pinhole	1.8 x 1.8 x 6 mm^3	R2486	0.67	0.8	7	1.4
Pinhole	1.8 x 1.8 x 6 mm^3	H8500	0.67	0.7	7	11
Pinhole	1.25 x 1.25 x 6 mm^3	H8500	0.67	0.8	4	11
Pinhole	1.8 x 1.8x 6 mm^3	M16	1	1.1	7	13
Pinhole	1.25x1.25x6 mm^3	M16	1	1.1	7	11
Pinhole	1.8x1.8x6 mm^3	M64	1	1.1	7	15
Pinhole	1.25x1.25x6 mm^3	M64	1	1.0	7	17

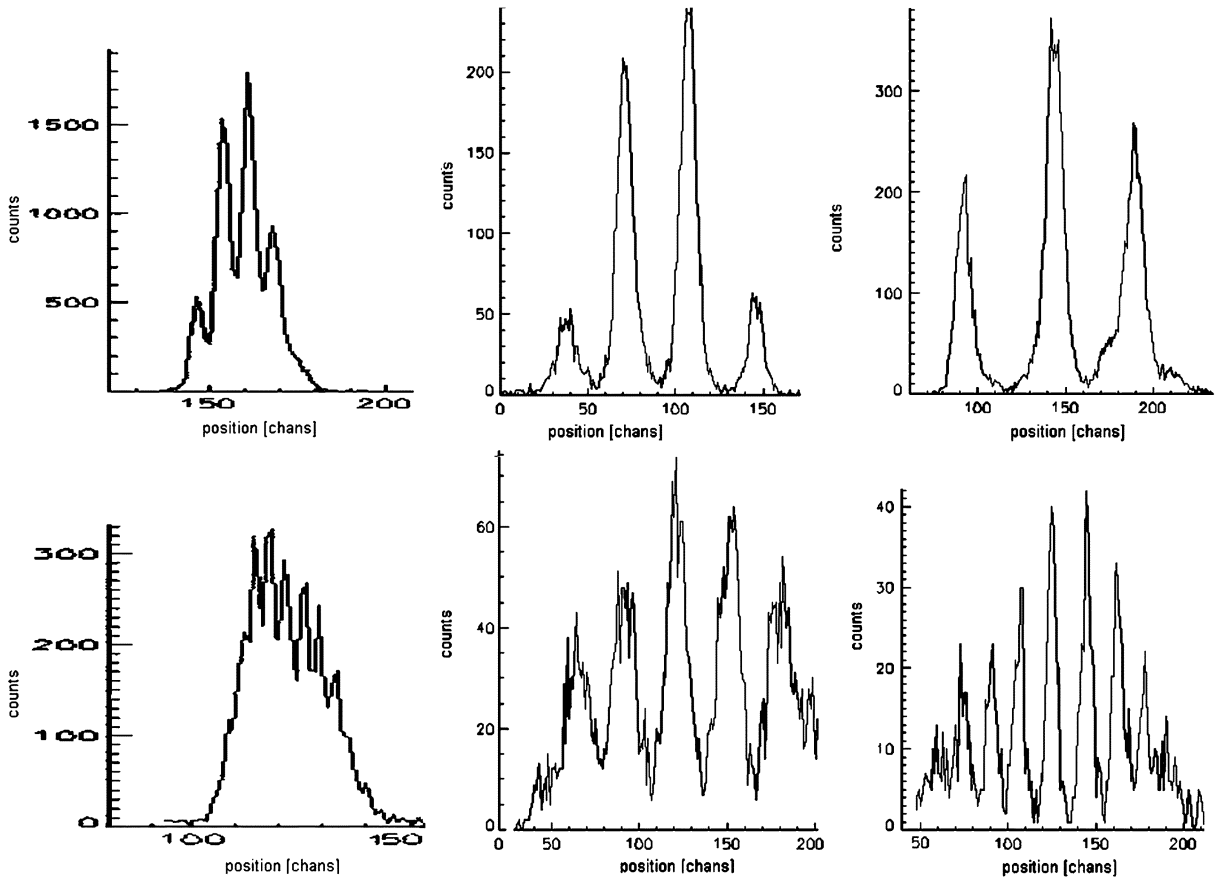

Fig. 5. Profiles obtained at 122 keV by irradiation of different scintillators (NaI(Tl) (a)–(c) $1.8 \times 1.8 \times 6$ mm^3 and (d)–(f) $1.25 \times 1.25 \times 5$ mm^3 coupled to different photodetectors: (a) and (d) R2486, (b) and (e) M16, and (c) and (f) M64.

would result in unacceptably wide dead regions. Fortunately, two other PSPMT types are now available from Hamamatsu: the H8500 (64 channels, 6×6 mm^2 anode pixel) and H9500 (256 channels, 3×3 mm^2 anode pixel). These PMTs have a larger active area and a smaller number of narrower dead regions are formed if an array is built. Fig. 6 shows a flood irradiation of two photodetectors using two different scintillator arrays coupled to a H8500 PSPMT. The pixel identification is good for the $1.8 \times 1.8 \times 6$ mm^3 array, but not as good for the $1.25 \times 1.25 \times 5$ mm^3 array (see also Table I). Fig. 7 shows the

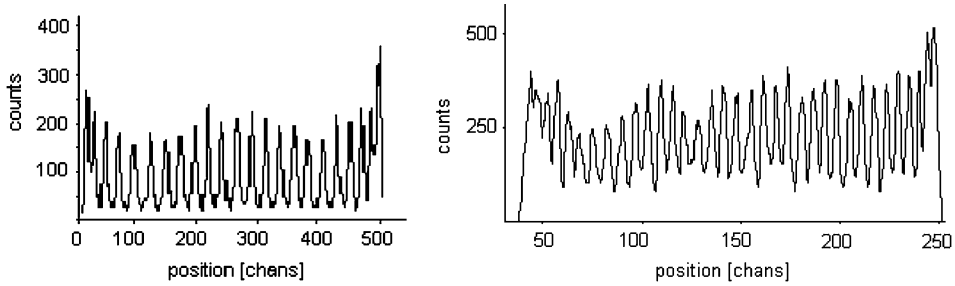

Fig. 6. Flood field irradiation (122 keV) of two NaI(Tl) scintillator arrays coupled to the H8500. The $1.8 \times 1.8 \times 6$ mm^3 pixels are well separated. For the $1.25 \times 1.25 \times 5$ mm^3, the separation is not as good.

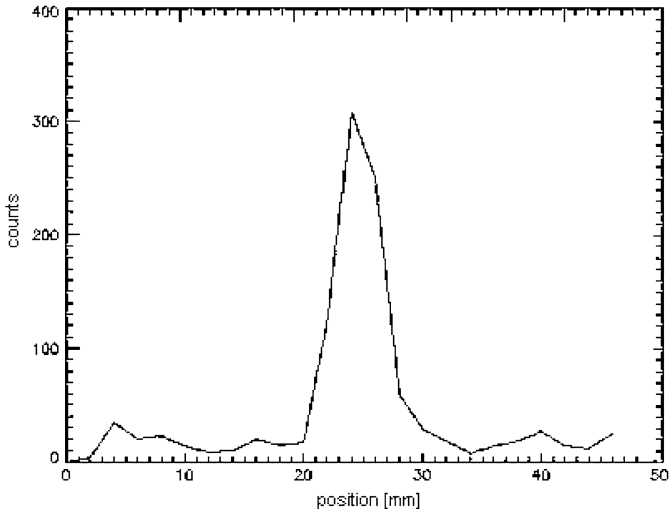

Fig. 7. Spatial resolution using a point source (122 keV, 1 mm diam), the used scintillator array is NaI(Tl) $1.8 \times 1.8 \times 6$ mm^3, coupled to the H8500. Tungsten pinhole (aperture $= 0.67$ mm). $M = 7$, FWHM $= 1.0$ mm. The improvement with respect to the R2486 is clear. Better intrinsic and total spatial resolution.

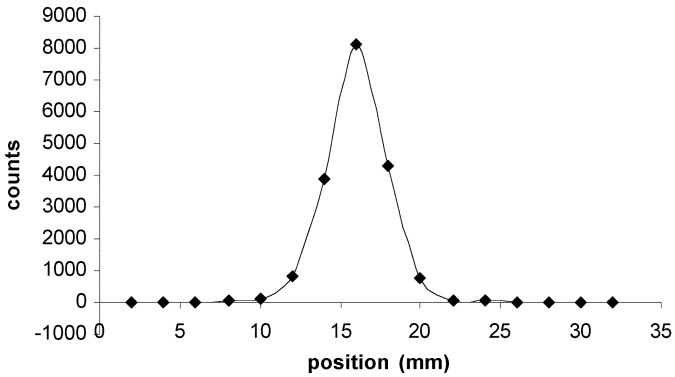

Fig. 8. Spatial resolution using a point source (122 keV, 1 mm diam) scintillator array (NaI(Tl) $1.25 \times 1.25 \times 5$ mm^3), coupled to the H8500. Tungsten pinhole (aperture $= 0.67$ mm). $M = 4$, FWHM $= 1.2$ mm. The improvement with respect to the R2486 is clear. Better intrinsic and total spatial resolution.

image of a point source (1 mm diameter) using the $1.8 \times 1.8 \times 6$ mm^3 array, with $M = 7$. Another measurement has been performed with the same setup but with magnification factor of $M = 3$ and $1.25 \times 1.25 \times 5$ mm^3 crystal pixel size (Fig. 8), to be compared with the coded aperture measurement (see next paragraph).

C. Increasing the Sensitivity: The Coded Aperture Option

1) Simulations: The system we have described does not allow dynamic studies because of low sensitivity. Different groups have proposed using multiple pinhole collimators to increase efficiency. Coded aperture collimators are another possible option [7]. For this reason a coded aperture was designed for use with our setup. Fig. 9 shows the coded aperture mask used (no-two-hole-touching, NTHT) [7], [9] modified uniformly redundant array (MURA) [8], [9], 22×22, thickness 1.5 mm, machinable tungsten. Fig. 9 shows also the preliminary results of pilot simulations.

Our preliminary results are indeed promising. The sensitivity is $\sim$30 times higher than that obtained with a single pinhole collimator. The theory of coded aperture signal-to-noise ratio (SNR) [7], [9] shows that this advantage is fully translated to an increase in the SNR only in the case of a point source. In the opposite limiting case of a uniform flood field, the SNR provided by a pinhole collimator is higher. The case of a hot spot with background activity, typical of many small animal imaging measurements, is intermediate to the two above extreme cases, but theoretical calculations, computer simulations, and previous experimental experience show that the increased sensitivity of coded apertures can actually translate to increased SNR, without sacrificing resolution [9].

2) Measurements—Preliminary Results: Measurements were made with a coded aperture collimator with a point-like gamma source (^{57} Co). Fig. 10 shows these initial results. Spatial resolution was determined starting from the FWHM of the Gaussian curved fitted to the count profiles through the maximum of the reconstructed peak. The result was 1.05 mm and 1.13 mm, along the x and y axis, respectively. These results need to be corrected for the finite dimensions of the point source used. Whereas we did not have direct access to this parameter, we note that the measured mean FWHM is consistent with submillimeter resolution for a source diameter of $\sqrt{1.09^2 - 1^2} = 434$ μm or more. System resolution can be estimated from the design parameters through the well-known equation

$$\lambda_s = \sqrt{\lambda_g^2 + \lambda_i^2} = \sqrt{\left(p_m \frac{1+M}{M}\right)^2 + \left(\frac{\text{FWHM}_i}{M}\right)^2} \quad (1)$$

where λ_g is the geometric resolution, λ_i the intrinsic resolution (both in image space), p_m the dimension of the apertures

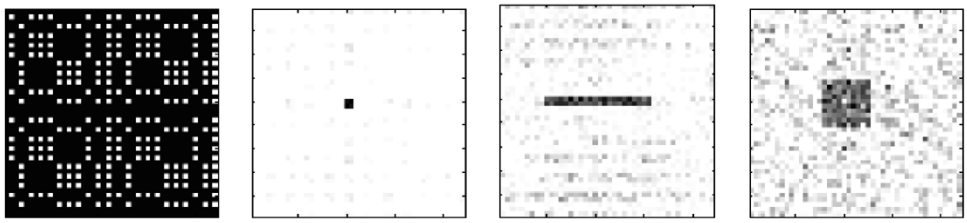

Fig. 9. Coded aperture used (at left) and images of different spatial distributions of the same activity (10 μCi) over the field of view: ideal point source, 1 cm line, and 5×5 mm^2 square. The acquisition time was 10 s in all cases, but for the square it was divided in two 5 s segments to allow for rotation of the aperture to mitigate near-field artifacts.

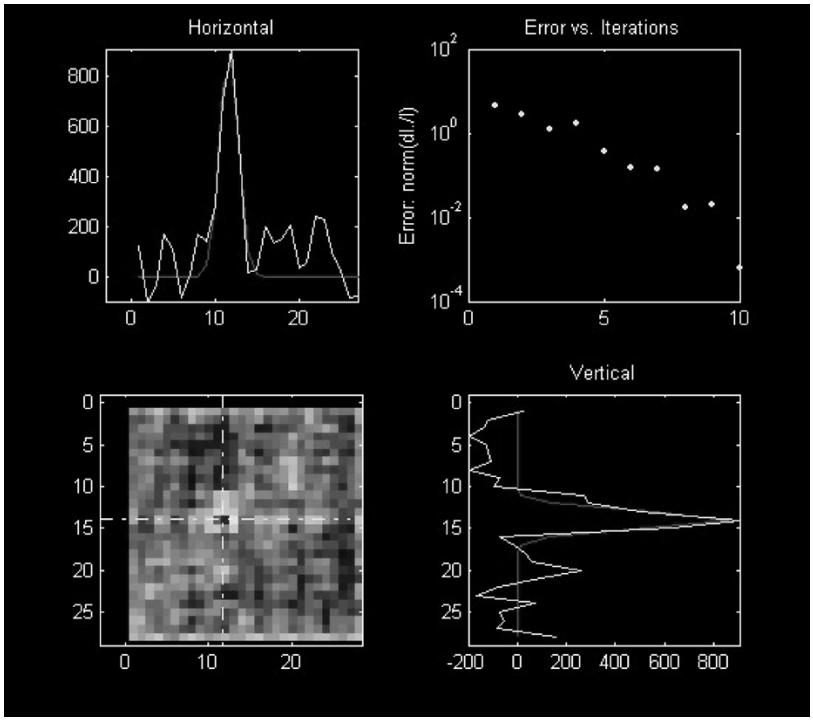

Fig. 10. Reconstruction of a 122 keV point-like source (1 mm diameter) using the coded apertures. Top-left: Horizontal profile of the reconstructed source. Top-right: The error in the resolution determination by iterative Gaussian fit. Bottom-left: Reconstructed image. Bottom-right: Vertical profile.

in the mask, and FWHM$_i$ the FWHM of the intrinsic response of the detector. Substituting $M = 4.13, p_m = 0.69$ mm, and FWHM$_i = 1.5$ mm, one gets $\lambda_s = 0.93$ mm. The increase in sensitivity has been estimated by comparison with the measurements performed with a pinhole collimator of approximately the same diameter as the holes in the coded aperture. An improvement of about 25 was measured. In fact, the sensitivity is, respectively, $\sim$ 40 cps/MBq (pinhole) and $\sim$ 1000 cps/MBq (coded aperture).

D. Outlook

Our plan is to improve detector performance through improvement of its intrinsic imaging properties, as well as through increase in its active size. Spatial resolution can be improved by using smaller pinholes or coded aperture holes, but in both cases better resolution would lead to a loss in sensitivity. We will test the newly available H9500 flat panel Hamamatsu PSPMT with 256 anode pads that has smaller anode pixel size (3×3 mm^3) than the current H8500 model, which should be optimal according to the measurement results shown in Table I. We can extrapolate from the measurements we have shown here that by using this PSPMT we will attain much better scintillation pixel identification and correspondingly substantially better spatial resolution. Furthermore, improving the pixel identification will allow us building arrays with four and more PSPMTs, without loss of response at the boundaries between the individual PSPMTs, practically with no dead area. Larger detector FOV would result in a larger imaging FOV or could be traded for the better spatial resolution at constant imaging FOV. In this case, the increased number of pixels results in better sampling capabilities, which in turn allow the use of a coded aperture with a larger number of holes, thus increasing sensitivity.

V. Conclusion

A desktop gamma imager system to perform *in vivo* imaging of small animals has been built and tested. Different scintillator arrays coupled to different pinhole collimators were used

with different photomultipliers. The optimal scintillator–photodetector combination was investigated. Simulations show that the detector efficiency can be greatly improved by using coded aperture collimation, which would potentially allow dynamic studies in those cases in which the sensitivity advantage translates to signal-to-noise ratio (SNR) advantage [7]. A coded aperture collimator was designed, built, and tested. The advantage in the increased sensitivity was verified experimentally.

Practical avenues for further improvement of imager performance were also analyzed. Spatial resolution performance of the photodetector can be improved by choosing a PSPMT with a smaller anode pad. The active detection area can be increased with an array of PSPMTs coupled to a single larger scintillator array. This future design has also the benefits of a larger field of view (FOV), while maintaining high and uniform spatial resolution, or of better resolution (at a constant FOV) if a higher magnification is used. The choice of the final detector layout will be driven both by scientific and practical consideration such as complexity and cost.

REFERENCES

[1] M. V. Green *et al.*, "High resolution PET, SPECT and projection imaging in small animals," *Comput. Med. Imaging Graph.*, vol. 25, pp. 79–86, 2001.

[2] B. Tsui *et al.*, "Evaluation of A-SPECT: A desktop pinhole SPECT system for small animal imaging," *IEEE Trans. Nucl. Sci.*, vol. 49, no. 5, pp. 2139–2147, Oct. 2002.

[3] M. Smith *et al.*, "Design of high sensitivity, high resolution, compact single photon imaging devices for small animal and dedicated breast imaging," presented at the IEEE 2001 Medical Imaging Conf. (MIC).

[4] N. Schramm *et al.*, "Development of a multipinhole detector for high sensitivity SPECT imaging," presented at the IEEE 2001 Medical Imaging Conf. (MIC).

[5] F. Garibaldi *et al.*, "Scintillator and photodetector array optimization for functional breast imaging," *NIM A*, vol. 497, pp. 51–59, 2003.

[6] F. Cusanno *et al.*, "Molecular imaging by single photon emission," presented at the Imaging Technologies in Biomedical Science (ITBS) Conf.

[7] E. E. Fenimore and T. Cannon, "Uniformly redundant arrays: Digital reconstruction methods," *Appl. Opt.*, vol. 20, no. 10, pp. 1858–1864, 1981.

[8] S. R. Gottesman and E. E. Fenimore, "New family of binary arrays for coded aperture imaging," *Appl. Opt.*, vol. 28, pp. 4344–4352, 1989.

[9] R. Accorsi, F. Gasparini, and R. C. Lanza, "A coded aperture for high resolution nuclear medicine planar imaging with a conventional Anger camera: Experimental results," *IEEE Trans. Nucl. Sci.*, vol. 48, no. 6, pp. 2411–2417, Dec. 2001.